Supported lysozyme for improved antimicrobial surface protection

Audrey Beaussart, Chloé Retourney, Fabienne Quilès, Raphael dos Santos Morais, Claire Gaiani, Henri-Pierre Fiérobe, Sofiane El-Kirat-Chatel

Journal of Colloid and Interface Science 582 (2021) 764–772

Supported Lysozyme for Improved Antimicrobial Surface Protection

Audrey Beaussart[1], Chloé Retourney[2], Fabienne Quilès[2], Raphael Dos Santos Morais[3], Claire Gaiani[3], Henri-Pierre Fiérobe[4] and Sofiane El-Kirat-Chatel[2*]

[1]Université de Lorraine, CNRS, LIEC, F-54000 Nancy, France

[2]Université de Lorraine, CNRS, LCPME, F-54000 Nancy, France

[3]Université de Lorraine, LIBio, F-54000, Nancy, France

[4]Aix Marseille Univ, CNRS, LCB, F-13420 Marseille, France

[*]Corresponding author:

Sofiane El-Kirat-Chatel: elkirat1@univ-lorraine.fr

Keywords: Antimicrobial surfaces; Lysozyme; Ligand-receptor grafting; Single-molecule force spectroscopy; *Micrococcus luteus*.

ToC.

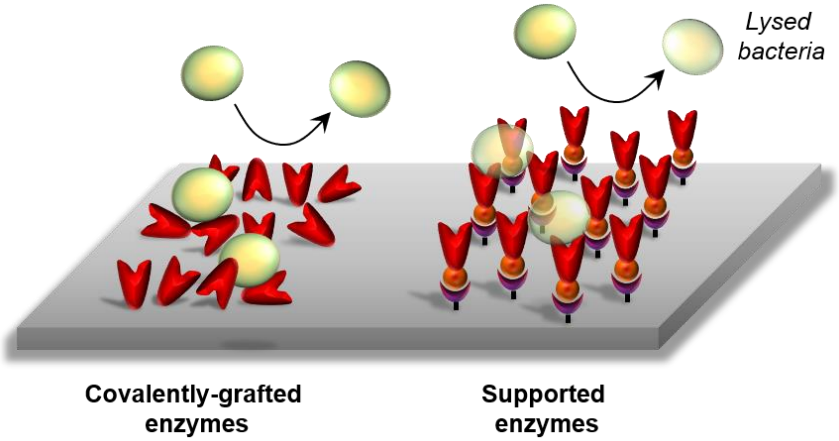

Authors' contributions: AB and SEKC design the research. AB, CR, FQ, RDSM, CG, H-PF and SEKC performed research. AB, CR, FQ, RDSM, CG, H-PF and SEKC analysed the data. AB and SEKC wrote the paper.

Abstract

Surface protection against biofilms is still an open challenge. Current strategies rely on coatings that are meant to guarantee antiadhesive or antimicrobial effects. While it seems difficult to ensure antiadhesion in complex media and against all the adhesive arsenal of microbes, strategies based on antimicrobials lack from sustainable functionalization methodologies to allow the perfect efficiency of the grafted molecules. Here we used the high affinity ligand-receptor interaction between biotin and streptavidin to functionalize surfaces with lysozyme, an enzyme that degrades the bacterial peptidoglycan cell wall. Biotinylated lysozyme was grafted on surfaces coated with streptavidin receptors. Using atomic force microscopy (AFM)-based single molecule force spectroscopy, we showed that grafting through ligand-receptor interaction allows the correct orientation of the enzyme on the substrate for enhanced activity towards the microbial target. The antibacterial efficiency was tested against *Micrococcus luteus* and revealed that surface protection was improved when lysozyme was grafted through the ligand-receptor interaction. These results suggest that bio-molecular interactions are promising for a sustainable grafting of antimicrobial agents on surfaces.

Introduction

Biofilm is a cooperative mode of life for microorganisms which can be formed on any type of substratum.[1] It consists of microbial communities adhered on a surface and embedded in a self-produced extracellular polymeric substance (EPS).[2] This three-dimensional organization leads to social and physical cellular interactions that make biofilm a totally different life-style from planktonic cells.[1] Microbes living in such consortium strongly adhere to the substrate and present an increased resistance to external stresses, rendering mature biofilms persistent and hard to eradicate.[3,4] In industry and human health, biofilm contaminations represent a major concern and are associated to important financial burdens and increased mortality.[3-6] Therefore, surface protection against biofilm is a great challenge in many applications and has mobilised important research efforts in the last decades.[7-10] Given the resistance of mature biofilms, their formation has to be tackled at the early stage, *i.e.* during the adhesion of pioneer bacteria. In that sense, different strategies aiming to obtain surfaces with antiadhesive or antimicrobial properties have been developed.[7,8,10,11] The former consists in modifying the physicochemical properties of the substrate to obtain an antifouling effect towards microorganisms. Although encouraging results have been obtained with polymers, *e.g.* polyethylene glycol, the protection efficiency was seen to decrease with time when surfaces were exposed to complex media.[7,10,12] For antimicrobial approaches, the principle is to functionalize surfaces with antimicrobial agents such as enzymes, antibiotics, antimicrobial peptides or disinfectants.[7,8,11] However, most antimicrobials offer a short-term protection and their leaching may be toxic and source of antimicrobial resistances.[13] Antimicrobial enzymes offer promising perspectives for surface protection as they can act continuously as long as their activity is preserved and they are less potent to trigger resistances.[14,15] Although their potentiality for surface protection is gaining more

and more interest, the functionalization method used to attach them on substrates is often a limiting step as they usually become less active once anchored to solid substrates due to *e.g.* steric hindrance, masking of their catalytic site, or denaturing interactions with the material.[16,17] Developing new functionalization methods overcoming these limitations is then crucial to exploit the possibility of using enzymes as efficient antimicrobial surface-protective agents. Attempts have been made to coat surfaces with DNase 1 or lysostaphin on polydopamine pre-coating, unfortunately resulting in a non-oriented distribution of the enzymes on the substrate.[18-20] Covalent grafting of lysozyme on stainless steel led also to surfaces with non-oriented enzymes.[21-23] Similarly, pluronic polymers were developed to graft lysozyme on surfaces but this methodology could not ensure the correct orientation of the enzyme on the substrate.[24] Peptidic linkers were used to graft lysostaphin in an oriented manner and to give molecular flexibility to the enzyme interacting with contaminating bacteria.[15] Although the method was original, the grafting strategy was based on weak interactions between the histidine tag and nickel-nitrilotriacetic acid or between silica binding peptide and glass.

The biotin-streptavidin interaction is one of the strongest noncovalent biomolecular bond known in nature.[25-28] Its high affinity (K_d of ~10^{-13} M) and stability make it of high interest for controlled and oriented molecular grafting.[25,29] Here, we took advantage of this high affinity ligand-receptor interaction to functionalize surfaces with lysozyme, an antibacterial enzyme that hydrolyses β-(1,4) linkages between N-acetylmuramic acid and N-acetyl-D-glucosamine residues of the peptidoglycan present in bacterial cell walls (Figure 1a).[30] We first demonstrate that enzymes are grafted in an oriented manner by probing the interaction between streptavidin surfaces and biotinylated lysozyme decorating atomic force microscopy (AFM) tips (Figure 1b). Then, we showed that lysozyme supported by the biotin-

streptavidin complex achieves greater antibacterial activity against the opportunistic pathogen *Micrococcus luteus*[31] than surfaces functionalized with covalently-bond lysozyme. This work demonstrates that grafting through bio-molecular interaction is a good strategy to prospect when developing coatings that bear oriented and preserved antimicrobials.

Results and discussion

Biotinylated lysozyme binds to streptavidin surfaces.

To preserve the antibacterial activity of the enzymes upon surface functionalization, biotinylated-lysozyme have been grafted through the ligand-receptor interaction between biotin and streptavidin (Figure 1a). For that, streptavidin was first covalently attached to gold surfaces. AFM topography images of the surface revealed that streptavidin coating was homogeneous and stable upon repeated scanning, indicating strong attachment of the receptor on the substrate (Figure 2). Scanning a small area at large forces removed the streptavidin layer and the scratched square was visible by imaging larger area at small forces. This allowed to determine that the streptavidin layer thickness was ~2 nm which correlates with previous thickness reported for streptavidin coated surfaces.[32] It also demonstrated that the first functionalization step resulted in a dense streptavidin layer which can be further used to graft biotinylated enzymes.

The second step of the grafting strategy consists in depositing biotinylated-lysozyme onto the streptavidin surface. We have assessed the amount of lysozyme attached to the surface in this way, and compared it to the amount of lysozyme when the enzyme is directly and covalently attached to the metal support. To do so, the concentration of absorbed proteins has been estimated *via* ultraviolet (UV)-visible spectroscopic quantification, revealing that lysozyme density was more than 4 times higher when directly grafted covalently on the surface (~59 $ng.mm^{-2}$ for covalently grafted lysozyme *vs* ~13 $ng.mm^{-2}$ for streptavidin-supported lysozyme).

The density of grafted streptavidin was ~27 ng.mm^{-2}. Regarding the molecular weights of biotinylated lysozyme and streptavidin (14300 and 52800 g.mol^{-1}, respectively), we obtain a respective molar density grafted on surfaces of ~9 x 10^{-13} mol.mm^{-2} and ~5 x 10^{-13} mol.mm^{-2}, corresponding to a molecular ratio of ~1.8, which is in good agreement with a stoichiometry of 2 expected for grafted streptavidin with biotinylated molecules (compared to the tetravalence of streptavidin in solution).[35]

Our hypothesis is that attaching lysozyme *via* receptor-ligand interaction allows to control the orientation of the enzyme on the surface. To verify this assumption, the specific binding of biotinylated-lysozyme to the streptavidin surface was assessed by single-molecule force spectroscopy (SMFS) measurements. For that, the adhesion frequency of the biotinylated-lysozyme-decorated tips toward streptavidin surface was quantified, and compared to the adhesion of other biotinylated or non-biotinylated molecules to the same support (Figure 1b). In details, approaching a functionalized tip from the streptavidin-coated surface results in a force-distance curves. On such curve, either the force remains close to zero independently of the distance, and the event is considered as non-adhesive, or the two proteins interact, which results in an increasing force until the link between the coated-tip and the streptavidin ruptures. The distance at which this link breaks informs on the extension/flexibility of the proteins. Figure 3 shows adhesion force and rupture length histograms, together with representative force curves, obtained between streptavidin surfaces and AFM tips functionalized with biotinylated lysozyme, non-biotinylated lysozyme and biotinylated albumin. The first bin corresponds to the frequency of non-adhesive events. The colours correspond to 3 independent measurements obtained with different coated-tips. For biotinylated lysozyme, 21 to 32 % of force curves presented simple peak adhesive events with unbinding forces ranging from 50 to 350 pN (mean value of 230±124 pN) and rupture lengths

from 5 to 100 nm (Figure 3a,b). Similar interactions were recorded for biotinylated albumin (Figure 3c,d). These values are in good accordance with previous SMFS studies on biotin-streptavidin interaction.[27,28,32-34] By contrast, most force curves featured no adhesive events when surfaces were probed with non-biotinylated lysozyme (adhesion frequency <7%, Figure 3e,f). This SMFS analysis demonstrates that, as expected, adhesion to the streptavidin pre-coated surface is modulated by the presence of a biotin group on the proteins (lysozyme and albumin). It confirms that biotin-streptavidin interaction can be used to graft lysozyme on surfaces in an oriented and specific manner.

To reinforce the idea that supported-lysozyme grafting preserves the conformation of the enzyme, we also performed infrared reflection absorption spectroscopy (IRRAS) on the different functionalized surfaces. This infrared-based technique allows chemical characterization of thin monolayers deposited on a metal surface. Figure 4 depicts the 1720-1600 cm^{-1} spectra, corresponding to the amide band I region and particularly sensitive to proteins secondary structures. The spectrum of streptavidin-coated surface (Fig. 4, black line) shows the occurrence of a band at 1637 cm^{-1} and a shoulder at 1686 cm^{-1} assigned to streptavidin β-sheet.[36] For the covalently-grafted lysozyme (Fig. 4, blue line) , the amide I band attributed to lysozyme was more intense as compared to the two other surfaces, with an integrated intensity 1.5 time higher than the other spectra. This result correlates with the higher protein amount on covalently-grafted lysozyme surfaces detected by (UV)-visible spectroscopy, although care should be taken in quantitative comparison as changes of proteins orientation may also influence the IRRAS spectra. The secondary structure of native lysozyme consists mainly in α-helices.[37] The amide I band of covalently grafted lysozyme showed a band near 1670 cm^{-1} (Fig. 4, blue line) instead of ~ 1650 cm^{-1} expected for the α-helix conformation. This shift may be attributed to a denaturation and/or aggregation of

lysozyme, as already described for heated lysozyme in solution,[38] and could result here from the covalent-grafting of lysozyme on the surface. Such alteration was not observed for the supported-lysozyme surface (Fig. 4, red line), for which the amide I band region showed two main bands at 1655 and 1638 cm^{-1} assigned to lysozyme α-helices and streptavidin β-sheets, respectively, consistent with the native conformations of both proteins. It confirms that supported-lysozyme grafting strategy favours a proper orientation of the lysozyme towards its target.

Next, we wanted to determine the capability of the different surfaces functionalized with enzymes to degrade bacterial cells.

Grafting lysozyme through biotin-streptavidin interaction preserves antibacterial activity. One advantage of using enzymes as antimicrobial agents is that they can degrade bacteria continuously as long as their activity is preserved. Therefore, enzyme stability is a prerequisite for long-term antibiofilm surface protection. An ideal antibacterial activity would eliminate contaminating bacteria and would be reusable, *i.e.* able to face repetitive contaminations. To test whether grafting through biotin-streptavidin improves the capability of lysozyme to face surface contamination, we have determined the antibacterial effect of different surfaces toward *M. luteus* by standard plating assays. Bacteria were exposed to surfaces and viability was determined over time and consecutive challenges (*i.e.* contamination with fresh bacteria). For consecutive challenges, ~5 x 10^7 bacteria were added on surfaces and viability was determined after 0h, 2h, 4h, 6h and 24h. After 24h, surfaces were rinsed and fresh bacteria were reloaded for the next challenge. Figure 5a shows the evolution of bacterial viability over 3 consecutives challenges on surfaces functionalized with streptavidin-supported biotinylated lysozyme, non-supported lysozyme and streptavidin alone. For control surfaces with streptavidin only, bacterial viability was ~100 % after 24h for all challenges. The slight decrease

observed upon time (<10 %) during the two first challenges could be attributed to bacteria adhering to the plastic well plates in which the surfaces are immersed to expose them to the cells. Surfaces functionalized with biotin-streptavidin-supported lysozyme killed 70-75 % of bacteria within 24h of all challenges. By contrast, the killing efficiency of surfaces with non-supported lysozyme decreased from 65 % to 50 % and 35 % during challenge 1, 2 and 3, respectively. During the 24h of challenge 1, bacterial concentration decreased constantly for both surfaces coated with lysozyme, yet with less efficiency for surfaces with non-supported lysozyme. While the killing efficiency remained constant over the 3 challenges for surfaces with biotin-streptavidin-supported lysozyme, it started to decrease during the challenge 2 and was almost abolished after the first 2h of challenge 3 for surfaces with non-supported lysozyme. This improved killing activity for lysozyme grafted by biotin-streptavidin interaction was confirmed up to 5 challenges (Fig. 5b). For clarity, only the bacterial survival values at 24h are indicated on Fig. 5b. The killing capacity of the supported-lysozyme surface after 5 challenges of 24h was ~55% (Fig. 5b, red dots) *versus* only ~20 % for surfaces with non-supported lysozyme (Fig. 5b, blue dots).

It could be argued that the decrease in antimicrobial performance is due to lysozyme removal during the rinsing steps. To exclude this hypothesis, we have analysed the topography of surfaces before and after the rinsing steps (Fig. S1). No significant difference in the height of the coating layer was observed after surface rinsing, suggesting that molecules grafted covalently or through the biotin-streptavidin interaction were not removed between the contamination challenges.

The bacterial killing capability of surfaces may decrease with time if enzyme activity decreases or if surfaces are fouled with bacterial debris. To determine the kinetics of bacterial killing by the different surfaces, the viability of ~1 x 10^8 bacteria was assessed over 7 days (Figure 6). On

surfaces bearing only streptavidin, bacterial viability remained constant at ~100 % over the total test duration. Surfaces functionalized with biotin-streptavidin-supported lysozyme killed ~75 % of bacteria after 24 h and 90 % after 3 days. By contrast, surfaces with non-supported lysozyme killed 60 % of bacteria after 24 h and a survival plateau was reached after 2 days with a maximum of 80 % of bacteria killed, suggesting that lysozyme was inactivated and/or not able to degrade bacteria after this time point. This improved antibacterial effect of surfaces with supported-lysozyme suggests that enzyme conformation and activity are preserved and that surface fouling by bacterial debris is less potent to inhibit enzymes grafted through biotin-streptavidin interaction.

To further demonstrate that ligand-receptor grafting improves the activity of grafted enzymes, we analysed the morphology of cells exposed to the different functionalized surfaces (Figure 7). As lysozyme degrades bacterial cell wall, we postulated that bacteria exposed to surfaces with preserved enzymatic activity would present more damages than bacteria exposed to surfaces with non-oriented enzymes or with streptavidin alone. Cells from the 5^{th} challenge (see above) were collected after 24 h of exposure to the different surfaces and deposited on gold substrates for AFM topographic imaging. Figure 7 shows low- and high-resolution images of *M. luteus* cells exposed to surfaces with streptavidin alone (Figure 7a), non-supported lysozyme (Figure 7b) and biotin-streptavidin supported lysozyme (Figure 7c). Large scale images revealed numerous aggregated cells for streptavidin surfaces whereas aggregates were smaller for the two surfaces functionalized with lysozyme, further confirming that the enzyme kills bacteria and decreases the cell density. At high resolution, all cells exposed to streptavidin surfaces presented smooth and regular cell walls (Figure 7a). By contrast, all cells exposed to surfaces with supported lysozyme presented substantial alterations of their structure and appeared bumped and rough (Figure 7c). Finally, two populations were

observed for cells exposed to surfaces with non-supported lysozyme: rough cells and smooth cells, documenting that lysozyme failed to degrade the cell wall of bacteria in this case. The potency of surfaces with supported lysozyme to degrade *M. luteus* cell wall as compared to surface with non-supported lysozyme was further confirmed through roughness calculation. Cells exposed to streptavidin, non-supported lysozyme and supported lysozyme presented roughness of 1.28 ± 0.43 nm, 3.06 ± 1.24 nm and 6.05 ± 3.05 nm, respectively (calculated on 12 cells from 3 independent experiments). This increased roughness directly reflects the activity of the enzyme on the bacterial cell wall and demonstrates that grafting through biotin-streptavidin interaction preserves lysozyme activity.

Altogether, these assays demonstrate an enhanced antimicrobial efficiency for the supported-lysozyme grafting strategy. As i) the supported-lysozyme surfaces performance cannot be attributed to a higher amount of enzymes, ii) the chemistry of the covalent grafting used for non-supported-lysozyme results in a random orientation of the protein on the surface with conformational changes and iii) the supported-lysozyme binds to the streptavidin-coated support *via* its biotin-group, the supported-lysozyme strategy most likely improves antibacterial surface protection by ensuring the correct orientation of enzymes on the surface, preserving enzyme conformation and limiting denaturing interactions with the substrate.

Conclusion

Surface protection against microbial biofilms remains an open challenge for which new strategies are needed.[4,6-10] In this work, we have demonstrated that the enzyme lysozyme could be grafted on surfaces in a manner that offers antimicrobial protection over consecutive contaminations. Our strategy is based on the strong-affinity bio-molecular ligand-receptor interaction -namely biotin-streptavidin- used here to support grafted enzymes and to improve

their activity against the bacteria *Micrococcus luteus*. Compared to previously reported approaches,[21-24] the supported-lysozyme surfaces showed improved antimicrobial protection over several days of continuous bacterial challenge. The efficiency of the bacterial killing effect as compared to surfaces coated with covalently-grafted lysozyme most likely arises from an improve orientation and conformation of the enzyme catalytic site towards its target, as demonstrated by AFM-based single molecule and IRRAS experiments.

Further developments of grafting strategies are under way to attach on the same surface various enzymes that would degrade diverse cell-wall components in order to reach a broad-spectrum activity. These results are encouraging for the future development of long-term surface protection by antimicrobial enzymes.

Materials and methods

Surface functionalization. Proteins were attached covalently on self-assembled monolayers (SAM) of carboxyl-terminated alkanethiols. Round glass coverslips (Ø12 mm) coated by plasma sputtering with a thin layer of chromium (~10 nm) and a thin layer of gold (~30 nm) were cleaned by UV-ozone treatment for 15 min, rinsed with ethanol and dried under N_2 flow. SAM were formed on clean surfaces by immersion overnight in a 1 mM solution containing 10% of 16-mercaptohexadecanoic acid (>90%, Sigma) and 90% of 11-mercapto-1-undecanol (>97%, Sigma) and then rinsed with ethanol and dried under N_2 flow. Carboxylic groups were activated by immersion for 30 min in a solution of 20 mg mL^{-1} N-hydroxysuccinimide (NHS, >97%, Sigma) and 50 mg mL^{-1} 1-ethyl-3-(3-dimethylaminopropyl)-carbodiimide (EDC, >99%, Sigma). Activated surfaces were rinsed in water and immersed for 2h with 0.2 mg mL^{-1} of streptavidin (>13 units/mg, Sigma) (for control surfaces functionalized with only streptavidin and for surfaces functionalized with supported lysozyme) or with 0.2 mg mL^{-1} of lysozyme

from chicken egg white (>90%, >40 units/mg, Sigma) (for surfaces functionalized with non-supported lysozyme) and then rinsed with phosphate-buffered saline (PBS, Sigma). For supported-lysozyme surfaces, streptavidin functionalized surfaces were further immersed for 30 min in 0.2 mg mL^{-1} of biotinylated lysozyme (>20 units/mg, Genetex) and rinsed again with PBS. All surfaces were prepared and used within the same day. For protein quantification, ultraviolet (UV)-visible measurements were performed in solution before and after deposition on the surfaces with a NanoDrop 2000c spectrophotometer (Thermo Fischer Scientific) and using molar extinction coefficients at 280 nm of 38940 and 41326 $M^{-1}.cm^{-1}$ and MWs of 14300 and 52800 $g.mol^{-1}$ for lysozyme and streptavidin, respectively.

AFM imaging and force spectroscopy. Unless stated otherwise, all AFM experiments were achieved in PBS at room temperature using a Bioscope Resolve AFM (Bruker corporation, Santa Barbara, CA). Before force measurements, surfaces functionalized with proteins were imaged with bare AFM tips (MSCT, Bruker) under minimal applied force. To measure streptavidin layer thickness, surfaces were first scratched with the AFM tip by applying large forces on an area of 1 x 1 μm^2 and then a larger area of 5 x 5 μm^2 was imaged under small forces. For force spectroscopy, gold coated AFM tips (NPG, Bruker) were functionalized with biotinylated lysozyme, biotinylated albumin (>80%, Sigma) or lysozyme following the same protocol as described for surfaces. Without dewetting, surfaces were immobilized in a glass-bottomed Petri dish with double side tape and covered with PBS. Force measurements were performed by recording 32 x 32 force-distance curves on areas of 1 x 1 μm^2 with a maximum applied force 250 pN, 200 ms contact time and a constant approach and retraction velocity of 1.5 µm s^{-1}. The spring constants of the cantilevers were measured by the thermal noise method. Adhesion force and rupture length histograms were obtained by calculating for each force curve the last adhesion peak and rupture distance. For cell imaging, 200 µl of cell

suspension from the challenge 5 were collected at 24h and deposited on gold substrates. After 2h, surfaces were gently rinsed by immersion in ultrapure water and dried overnight at 30°C before imaging in peak-force tapping mode using a gold-coated AFM tips (NPG, nominal spring constant 0.24 N/m, Bruker corporation) on a Fastscan Dimension-Icon AFM (Bruker corporation, Santa Barbara, CA). Rms (root mean square) roughness values correspond to the Rq values given by the Nanoscopy analysis software on 400 nm x 400 nm square at the surface of the bacteria after 2nd-order-flattening of the height image. Given values have been averaged over at least 12 bacteria per conditions.

Bacterial growth and viability tests. *M. luteus* ATCC4698 cells were grown routinely on Luria-Bertani (LB, Sigma) plates at 30°C. For viability experiments, a single colony of *M. luteus* was grown in 5 mL of LB at 30°C with shaking at 200 rpm. Overnight cultures were harvested by centrifugation at 5000 *g* for 5 min, washed twice in PBS. For consecutive challenges, 1.2 mL of bacterial suspension containing ~5 x 10^7 bacteria were deposited on functionalized surfaces in 12-well plates and gently agitated at 30°C. At defined time points (0h, 2h, 4h, 6h and 24h), 100 µl were pipetted, serially diluted and plated on LB before cultivation at 30°C to determine bacterial viability. Before reloading with 1.2 mL of fresh bacteria for the next challenge, surfaces were gently rinsed in 3 baths of PBS. For continuous experiments without bacterial reload, 2 mL of bacterial suspension containing ~1 x 10^8 bacteria were deposited on surfaces and 50 µL were pipetted at different time points (from 0 to 7 days) for viability analysis. Results presented for viability tests correspond to three independent experiments.

Infrared reflection absorption spectroscopy (IRRAS). Infrared spectra were recorded in the mid-infrared range on a Bruker Vertex 70v spectrometer equipped with a KBr beamsplitter and a MCT detector. An advanced grazing angle specular reflectance accessory (Pike technologies Inc.) with a fixed 80° angle of incidence was used for acquiring spectra of the

functionalized gold-coated surfaces. The spectra resolution was 4 cm^{-1} and the accumulation time was ~ 2.5 min (256 scans). Compartments containing the detector and the specular reflectance accessory were under vacuum (< 1 hPa). IR spectra are displayed in the scale corresponding to log (1/R), where R is the collected reflectance.

Acknowledgements

This work has received financial support from the CNRS through the MITI interdisciplinary program and from the French PIA project "Lorraine Université d'Excellence", reference ANR-15-IDEX-04-LUE. S.E.K.C is a CRCN researcher at the CNRS. The authors thank the Spectroscopy and Microscopy Service Facility (SMI) of LCPME (Université de Lorraine-CNRS) where AFM and IRRAS experiments were performed. Sylvie Derclaye from the Catholic University of Louvain is acknowledged for gold surface deposition.

Conflict of interest

The authors declare no conflict of interest.

References

[1] H.C. Flemming, J. Wingender, U. Szewzyk, P. Steinberg, S.A. Rice, S. Kjelleberg, Biofilms: an emergent form of bacterial life, Nat Rev Microbiol 14 (2016), 563-575, https://doi.org/10.1038/nrmicro.2016.94.

[2] H.C. Flemming, J. Wingender, The biofilm matrix, Nat Rev Microbiol 8 (2010), 623-633, https://doi.org/10.1038/nrmicro2415.

[3] J.W. Costerton, P.S. Stewart, E.P. Greenberg, Bacterial biofilms: a common cause of persistent infections, Science 284 (1999), 1318-1322, https://doi.org/10.1126/science.284.5418.1318.

[4] L. Hall-Stoodley, J.W. Costerton, P. Stoodley, Bacterial biofilms: from the natural environment to infectious diseases, Nat Rev Microbiol 2 (2004), 95-108, https://doi.org/10.1038/nrmicro821.

[5] V. Carniello, B.W. Peterson, H.C. van der Mei, H.J. Busscher, Physico-chemistry from initial bacterial adhesion to surface-programmed biofilm growth, Adv Colloid Interface Sci 261 (2018), 1-14, https://doi.org/10.1016/j.cis.2018.10.005.

[6] H.C. Flemming, S. Wuertz, Bacteria and archaea on Earth and their abundance in biofilms, Nat Rev Microbiol 17 (2019), 247-260, https://doi.org/10.1038/s41579-019-0158-9.

[7] D. Alves, M. Olivia Pereira, Mini-review: Antimicrobial peptides and enzymes as promising candidates to functionalize biomaterial surfaces, Biofouling 30 (2014), 483-499, https://doi.org/10.1080/08927014.2014.889120.
[8] K. Glinel, P. Thebault, V. Humblot, C.M. Pradier, T. Jouenne, Antibacterial surfaces developed from bio-inspired approaches, Acta Biomater 8 (2012), 1670-1684, https://doi.org/10.1016/j.actbio.2012.01.011.
[9] E.O. Ogunsona, R. Muthuraj, E. Ojogbo, O. Valerio, T.H. Mekonnen, Engineered nanomaterials for antimicrobial applications: A review, Applied Materials Today 18 (2020), 1-32, https://doi.org/10.1016/j.apmt.2019.100473.
[10] C. von Eiff, B. Jansen, W. Kohnen, K. Becker, Infections associated with medical devices: pathogenesis, management and prophylaxis, Drugs 65 (2005), 179-214, https://doi.org/10.2165/00003495-200565020-00003.
[11] D. Campoccia, L. Montanaro, C.R. Arciola, A review of the biomaterials technologies for infection-resistant surfaces, Biomaterials 34 (2013), 8533-8554, https://doi.org/10.1016/j.biomaterials.2013.07.089.
[12] A. Roosjen, W. Norde, H.C. van der Mei, H.J. Busscher, The Use of Positively Charged or Low Surface Free Energy Coatings versus Polymer Brushes in Controlling Biofilm Formation, Progr Colloid Polym Sci 132 (2006), 138-144, https://doi.org/DOI 10.1007/2882_026.
[13] H. Murata, R.R. Koepsel, K. Matyjaszewski, A.J. Russell, Permanent, non-leaching antibacterial surface--2: how high density cationic surfaces kill bacterial cells, Biomaterials 28 (2007), 4870-4879, https://doi.org/10.1016/j.biomaterials.2007.06.012.
[14] B. Thallinger, E.N. Prasetyo, G.S. Nyanhongo, G.M. Guebitz, Antimicrobial enzymes: an emerging strategy to fight microbes and microbial biofilms, Biotechnol J 8 (2013), 97-109, https://doi.org/10.1002/biot.201200313.
[15] X. Wu, K. Fraser, J. Zha, J.S. Dordick, Flexible Peptide Linkers Enhance the Antimicrobial Activity of Surface-Immobilized Bacteriolytic Enzymes, ACS Appl Mater Interfaces 10 (2018), 36746-36756, https://doi.org/10.1021/acsami.8b14411.
[16] T. Cha, A. Guo, X.Y. Zhu, Enzymatic activity on a chip: the critical role of protein orientation, Proteomics 5 (2005), 416-419, https://doi.org/10.1002/pmic.200400948.
[17] Y. Liu, T.L. Ogorzalek, P. Yang, M.M. Schroeder, E.N. Marsh, Z. Chen, Molecular orientation of enzymes attached to surfaces through defined chemical linkages at the solid-liquid interface, J Am Chem Soc 135 (2013), 12660-12669, https://doi.org/10.1021/ja403672s.
[18] D. Alves, A. Magalhaes, D. Grzywacz, D. Neubauer, W. Kamysz, M.O. Pereira, Co-immobilization of Palm and DNase I for the development of an effective anti-infective coating for catheter surfaces, Acta Biomater 44 (2016), 313-322, https://doi.org/10.1016/j.actbio.2016.08.010.
[19] J.J.T.M. Swartjes, T. Das, S. Sharifi, G. Subbiahdoss, P.K. Sharma, B.P. Krom, H.K. Busscher, H.C. van der Mei, A Functional DNase I Coating to Prevent Adhesion of Bacteria and the Formation of Biofilm, Advanced Functional Materials 23 (2013), 2843-2849, https://doi.org/10.1002/adfm.201202927.
[20] G. Yeroslavsky, O. Girshevitz, J. Foster-Frey, D.M. Donovan, S. Rahimipour, Antibacterial and antibiofilm surfaces through polydopamine-assisted immobilization of lysostaphin as an antibacterial enzyme, Langmuir 31 (2015), 1064-1073, https://doi.org/10.1021/la503911m.
[21] A. Caro, V. Humblot, C. Methivier, M. Minier, L. Barbes, J. Li, M. Salmain, C.M. Pradier, Bioengineering of stainless steel surface by covalent immobilization of enzymes. Physical characterization and interfacial enzymatic activity, J Colloid Interface Sci 349 (2010), 13-18, https://doi.org/10.1016/j.jcis.2009.12.001.

[22] A. Caro, V. Humblot, C. Methivier, M. Minier, M. Salmain, C.M. Pradier, Grafting of lysozyme and/or poly(ethylene glycol) to prevent biofilm growth on stainless steel surfaces, J Phys Chem B 113 (2009), 2101-2109, https://doi.org/10.1021/jp805284s.
[23] M. Minier, M. Salmain, N. Yacoubi, L. Barbes, C. Methivier, S. Zanna, C.M. Pradier, Covalent immobilization of lysozyme on stainless steel. Interface spectroscopic characterization and measurement of enzymatic activity, Langmuir 21 (2005), 5957-5965, https://doi.org/10.1021/la0501278.
[24] A.K. Muszanska, H.J. Busscher, A. Herrmann, H.C. van der Mei, W. Norde, Pluronic-lysozyme conjugates as anti-adhesive and antibacterial bifunctional polymers for surface coating, Biomaterials 32 (2011), 6333-6341, https://doi.org/10.1016/j.biomaterials.2011.05.016.
[25] C.E. Chivers, E. Crozat, C. Chu, V.T. Moy, D.J. Sherratt, M. Howarth, A streptavidin variant with slower biotin dissociation and increased mechanostability, Nat Methods 7 (2010), 391-393, https://doi.org/10.1038/nmeth.1450.
[26] D.E. Hyre, I. Le Trong, E.A. Merritt, J.F. Eccleston, N.M. Green, R.E. Stenkamp, P.S. Stayton, Cooperative hydrogen bond interactions in the streptavidin-biotin system, Protein Sci 15 (2006), 459-467, https://doi.org/10.1110/ps.051970306.
[27] F. Rico, A. Russek, L. Gonzalez, H. Grubmuller, S. Scheuring, Heterogeneous and rate-dependent streptavidin-biotin unbinding revealed by high-speed force spectroscopy and atomistic simulations, Proc Natl Acad Sci U S A 116 (2019), 6594-6601, https://doi.org/10.1073/pnas.1816909116.
[28] J.M. Teulon, Y. Delcuze, M. Odorico, S.W. Chen, P. Parot, J.L. Pellequer, Single and multiple bonds in (strept)avidin-biotin interactions, J Mol Recognit 24 (2011), 490-502, https://doi.org/10.1002/jmr.1109.
[29] O.H. Laitinen, V.P. Hytonen, H.R. Nordlund, M.S. Kulomaa, Genetically engineered avidins and streptavidins, Cell Mol Life Sci 63 (2006), 2992-3017, https://doi.org/10.1007/s00018-006-6288-z.
[30] M. Derde, V. Vie, A. Walrant, S. Sagan, V. Lechevalier, C. Guerin-Dubiard, S. Pezennec, M.F. Cochet, G. Paboeuf, M. Pasco, F. Baron, M. Gautier, S. Jan, F. Nau, Antimicrobial activity of lysozyme isoforms: Key molecular features, Biopolymers 107 (2017), https://doi.org/10.1002/bip.23040.
[31] S. Lee, Y.W. An, C.H. Choi, M.R. Yun, S. Kim, H. Cheong, Y.S. Choi, D.W. Kim, Complete Genome Sequences of Micrococcus luteus Strains NCCP 15687 and NCCP 16831, Isolated in South Korea, Microbiol Resour Announc 9 (2020), https://doi.org/10.1128/MRA.01558-19.
[32] M. Kohler, A. Karner, M. Leitner, V.P. Hytonen, M. Kulomaa, P. Hinterdorfer, A. Ebner, pH-dependent deformations of the energy landscape of avidin-like proteins investigated by single molecule force spectroscopy, Molecules 19 (2014), 12531-12546, https://doi.org/10.3390/molecules190812531.
[33] G.U. Lee, D.A. Kidwell, R.J. Colton, Sensing Discrete Streptavidin-Biotin Interactions with Atomic Force Microscopy, Langmuir 10 (1994), 354-357, https://doi.org/10.1021/la00014a003.
[34] Y.S. Lo, N.D. Huefner, W.S. Chan, F. Stevens, J.M. Harris, T.P. Beebe, Specific Interactions between Biotin and Avidin Studied by Atomic Force Microscopy Using the Poisson Statistical Analysis Method, Langmuir 15 (1999), 1373-1382, https://doi.org/10.1021/la981003g.
[35] G.V. Dubacheva, C. Araya-Callis, A. Geert Volbeda, M. Fairhead, J. Codee, M. Howarth, R.P. Richter, Controlling Multivalent Binding through Surface Chemistry: Model Study on Streptavidin, J Am Chem Soc 139 (2017), 4157-4167, https://doi.org/10.1021/jacs.7b00540.

[36] A. Krüger, A. Bürkle, A. Mangerich, K. Hauser, A combined approach of surface passivation and specific immobilization to study biomolecules by ATR-FTIR spectroscopy, Biomed Spectrosc Imaging 7 (2018), 25-33, https://doi.org/10.3233/BSI-180174.
[37] G. Thakur, R.M. Leblanc, Conformation of lysozyme Langmuir monolayer studied by infrared reflection absorption spectroscopy, Langmuir 25 (2009), 2842-2849, https://doi.org/10.1021/la803233p.
[38] P. Sassi, A. Giugliarelli, M. Paolantoni, A. Morresi, G. Onori, Unfolding and aggregation of lysozyme: a thermodynamic and kinetic study by FTIR spectroscopy, Biophys Chem 158 (2011), 46-53, https://doi.org/10.1016/j.bpc.2011.05.002.

452 **Figures**

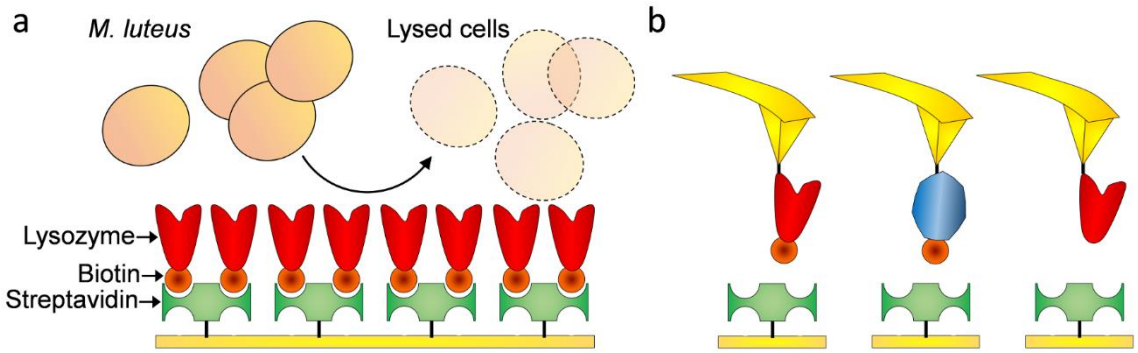

453

454 **Figure 1. Principle of surface protection with biotin-streptavidin grafted enzymes and of**
455 **single-molecule force spectroscopy.** (a) Lysozyme was grafted on surface through biotin-
456 streptavidin interaction to obtain antimicrobial surfaces. Streptavidin was covalently attached
457 to carboxyl-terminated surfaces *via* NHS/EDC chemistry and biotinylated lysozyme was added.
458 When bacterial cells, here *M. luteus*, approach the surface, the supported lysozyme degrades
459 their cell wall, leading to bacterial death. (b) To demonstrate the specific interaction between
460 biotin and streptavidin, AFM tips were functionalized with biotinylated lysozyme (left),
461 biotinylated albumin (center) and non-tagged lysozyme (right) and probed towards
462 streptavidin surfaces.

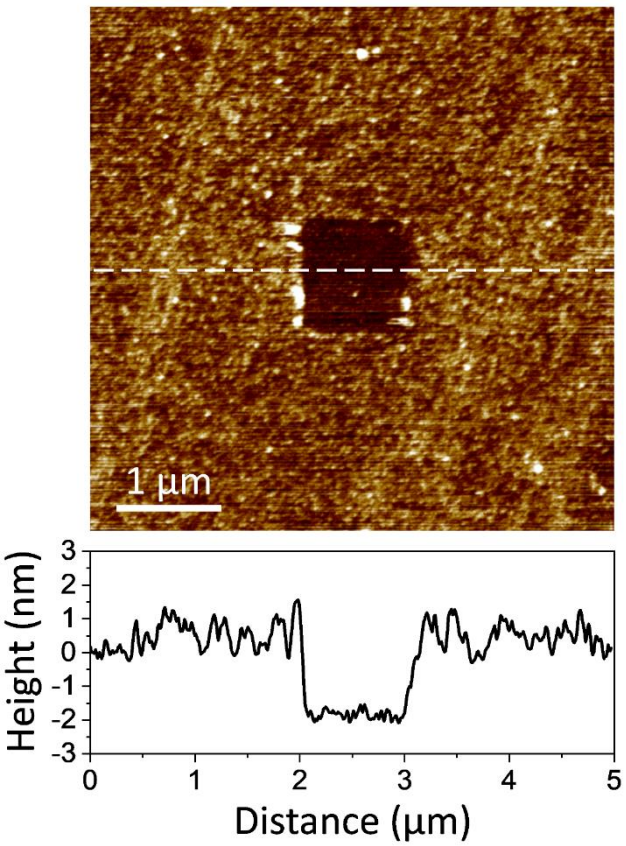

Figure 2. Topography of streptavidin surfaces. AFM height image (5 x 5 µm²; z scale = 8 nm) of a surface with covalently attached streptavidin showing a smooth and homogeneous topography. A vertical cross section taken along the dashed line is shown below the image. The streptavidin thickness (~2 nm) was determined by imaging a square area of 1 x 1 µm² at large forces (>10 nN) before imaging 5 x 5 µm² of the same area at small forces.

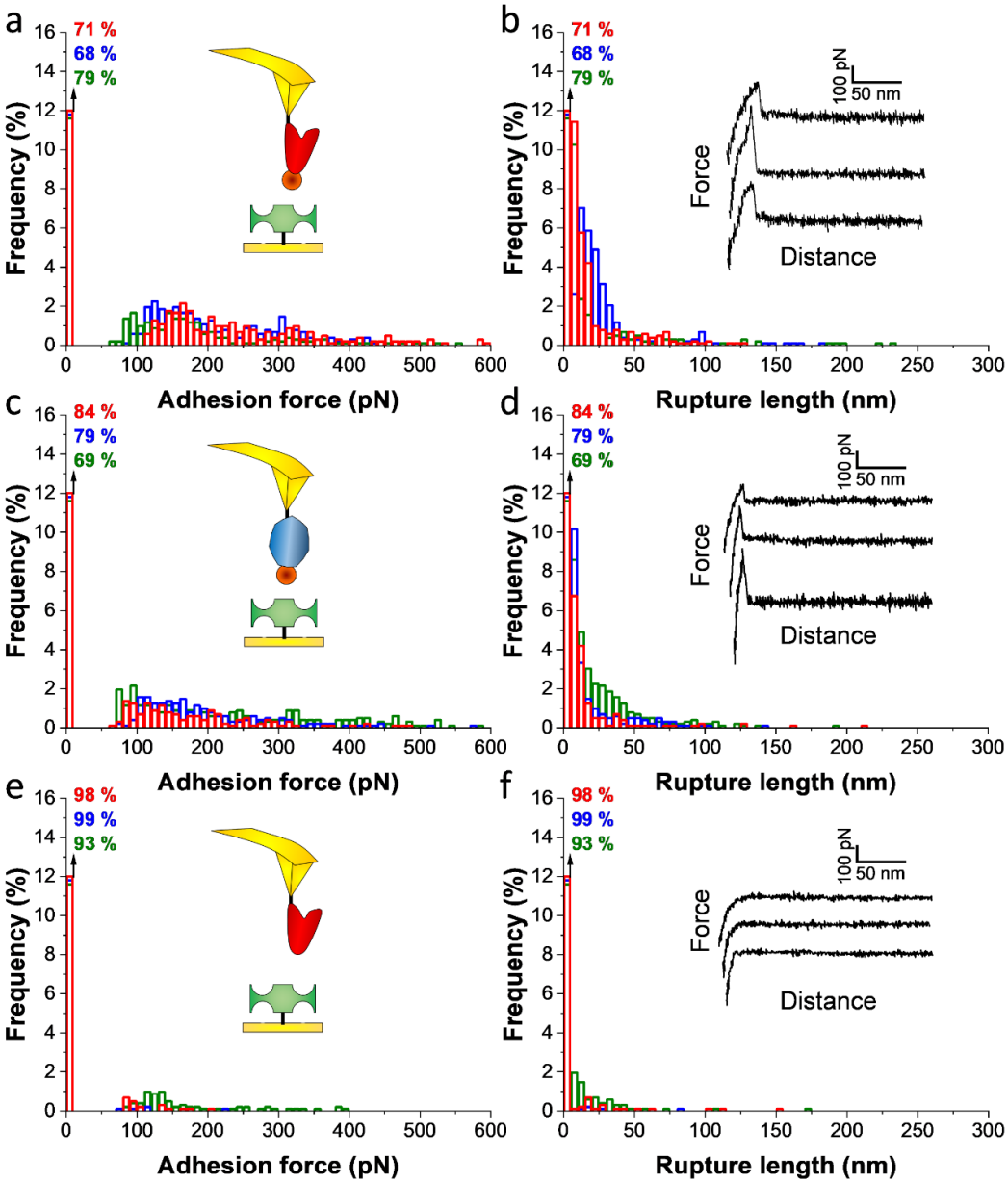

Figure 3. Single-molecule force spectroscopy demonstrates specific interaction between streptavidin surface and biotinylated proteins. Adhesion force (a, c, e) and rupture length histograms together with representative force curves (b, d, f), obtained by recording force-volume maps of 32 x 32 pixels on areas of 1 × 1 µm² between streptavidin surfaces and AFM tips bearing biotinylated lysozyme (a, b), biotinylated albumin (c, d) and non-tagged lysozyme (e, f). Blue, red and green colours correspond to the adhesion frequency (calculated from 1024 force-curves each) from 3 independent experiments using different functionalized tips. The numbers on top of the first bin indicate the number of non-adhesive events for each tip.

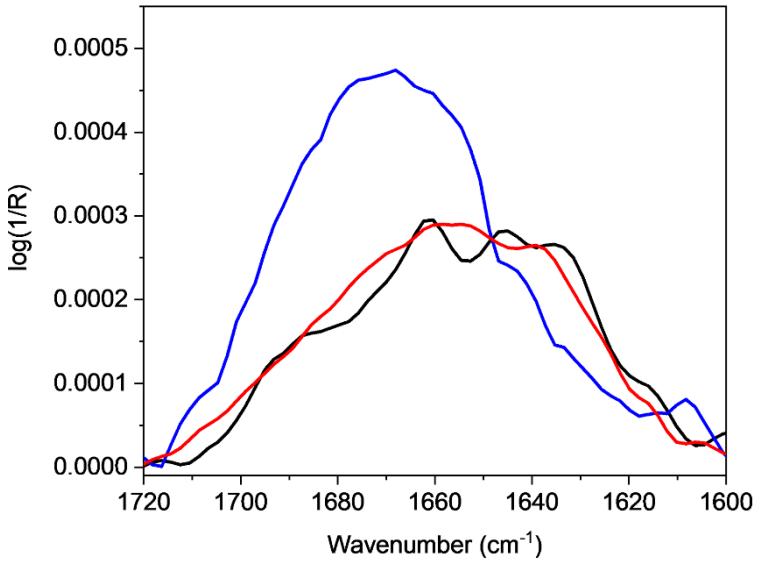

479

480 **Figure 4. IRRAS spectra of functionalized surfaces.** Amide I band region (1720-1600 cm^{-1}) of
481 gold surfaces functionalized with streptavidin (black line), lysozyme by covalent grafting (blue
482 line) and biotin-streptavidin-supported lysozyme (red line).

483

484

485

486

487

488

489

490

491

492

493

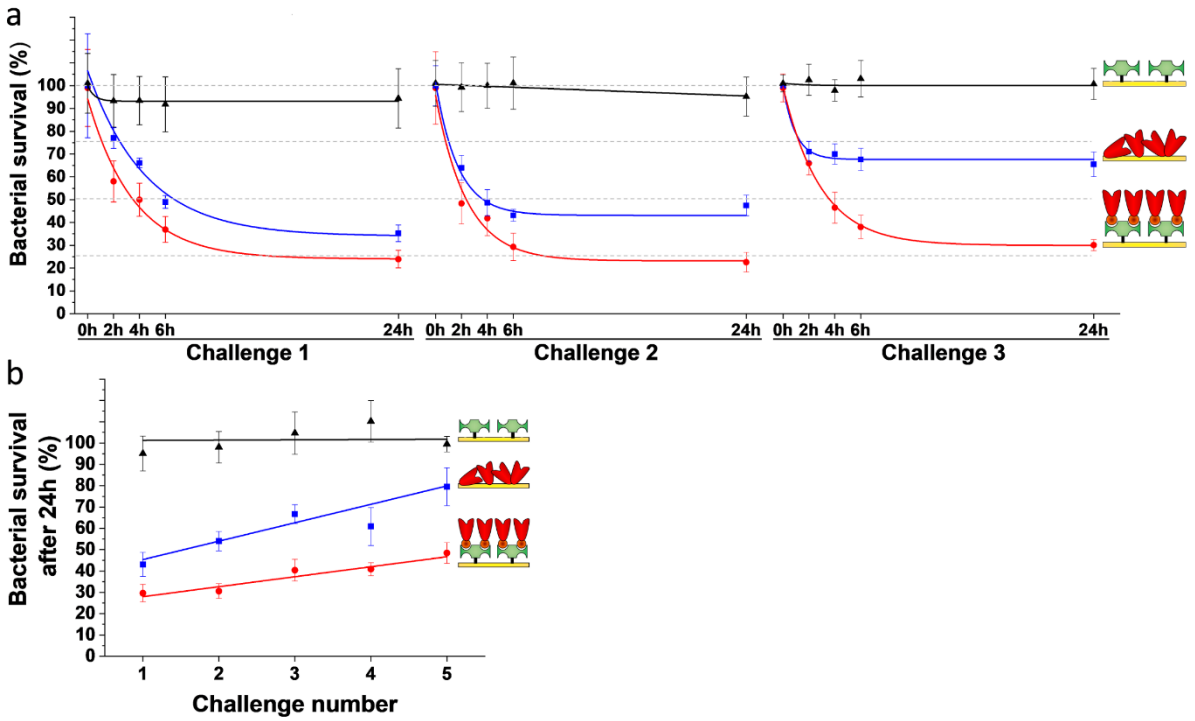

Figure 5. Antimicrobial activity of surfaces with supported lysozyme is preserved over consecutive challenges. (a) Viability of *M. luteus* cells determined by counting the number of colony forming units (CFU) on plates after 3 consecutive challenges of 24 h on surfaces functionalized with streptavidin (black triangles), non-supported lysozyme (blue squares) and streptavidin-supported biotinylated lysozyme (red disks). For each challenge, viability was determined after (a) 0 h, 2 h, 4 h, 6 h and 24 h and (b) 24 h exposure time, then surfaces were rinsed and fresh cells were reloaded. Bacterial survivals decrease exponentially, as revealed by the exponential decay fit (plain lines). (b) Values of bacterial survival after 24h for surfaces exposed to 5 consecutive challenges. Plain lines have not physical meaning, they are depicted for eye guidance, highlighting the clear capacity of supported-lysozyme surface to handle multiple contaminations. Experimental values correspond to the average over 3 experiments. Errors bars indicate the standard deviation between experiments.

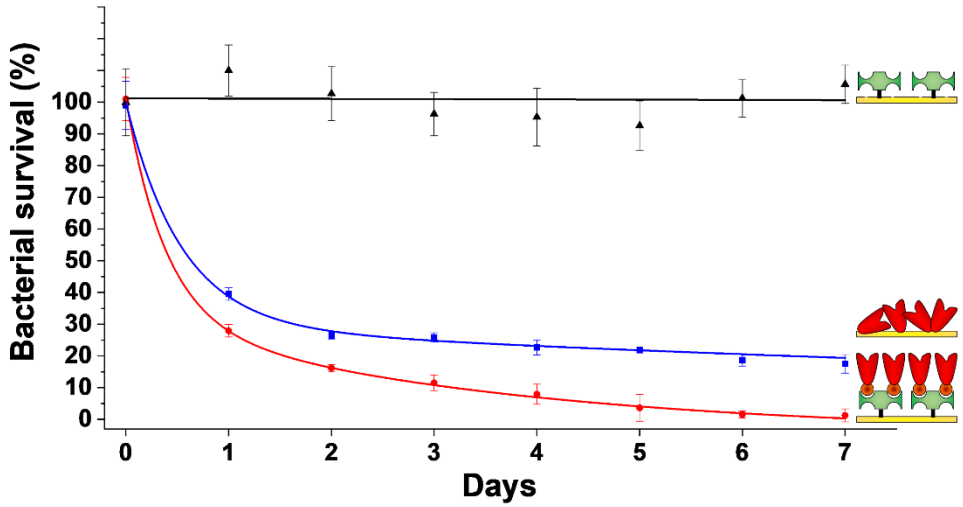

Figure 6. Antimicrobial activity of surfaces with supported lysozyme is preserved during continuous challenge. Viability of *M. luteus* cells determined each 24 h over 7 days by counting the number of colony forming units (CFU) on plates after exposure to surfaces functionalized with streptavidin (black triangles), non-supported lysozyme (blue squares) and streptavidin-supported biotinylated lysozyme (red disks). Experimental values correspond to the average over 3 experiments. Errors bars indicate the standard deviation between experiments.

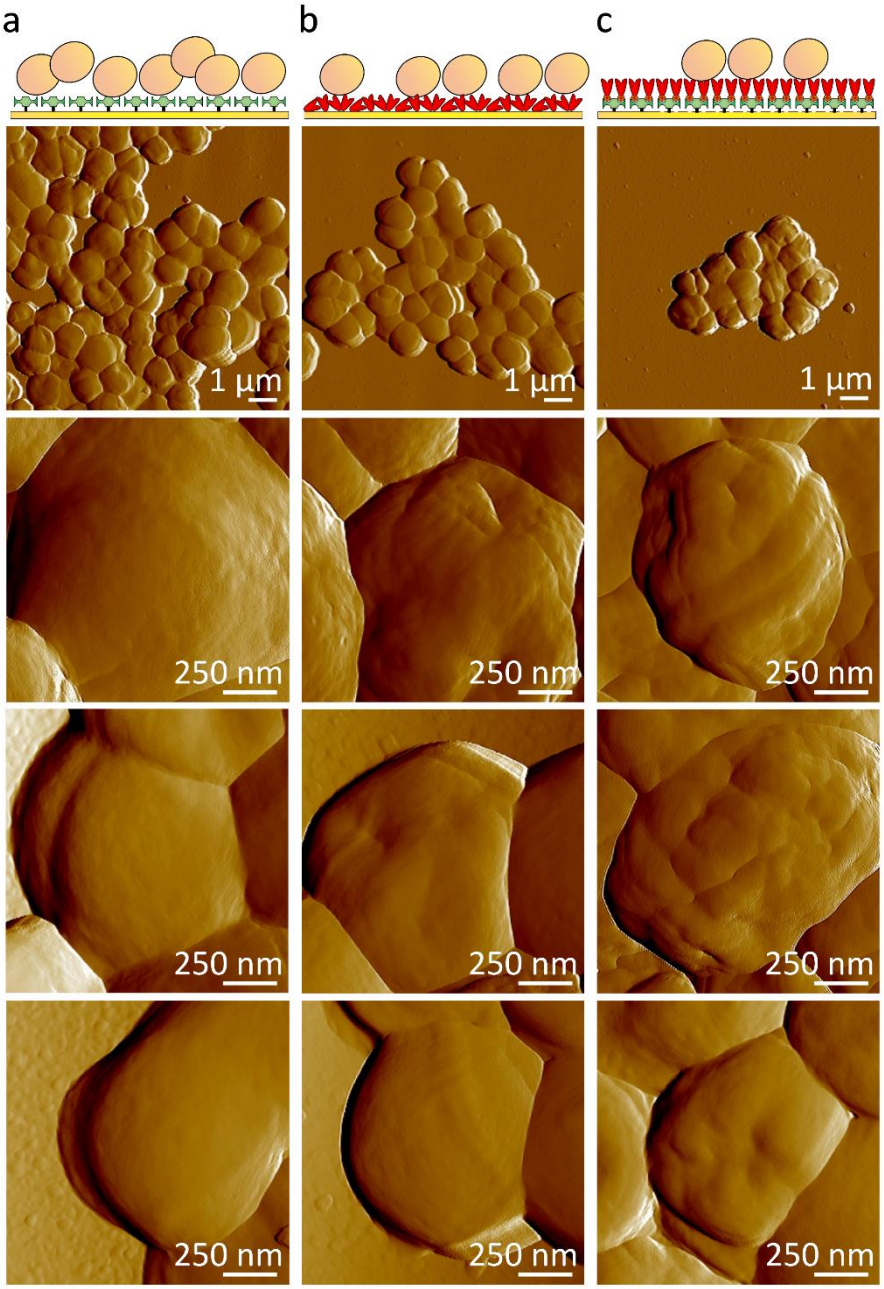

518

519 **Figure 7. AFM imaging reveals structural damages on cells exposed to surfaces with**
520 **supported lysozyme.** Low and high resolution peak force error images of *M. luteus* cells
521 collected from the 5th challenge after 24 h of exposure. (a) Cells exposed to surfaces with
522 streptavidin alone, (b) cells exposed to surface with non-supported lysozyme and (c) cells
523 exposed to surfaces with biotin-streptavidin supported lysozyme. High resolution images
524 correspond to cells from 3 independent experiments. Similar images have been obtained for
525 at least 12 bacteria per condition.

526

Supplementary Information

Supported Lysozyme for Improved Antimicrobial Surface Protection

Audrey Beaussart, Chloé Retourney, Fabienne Quilès, Raphael Dos Santos Morais, Claire Gaiani, Henri-Pierre Fiérobe and Sofiane El-Kirat-Chatel

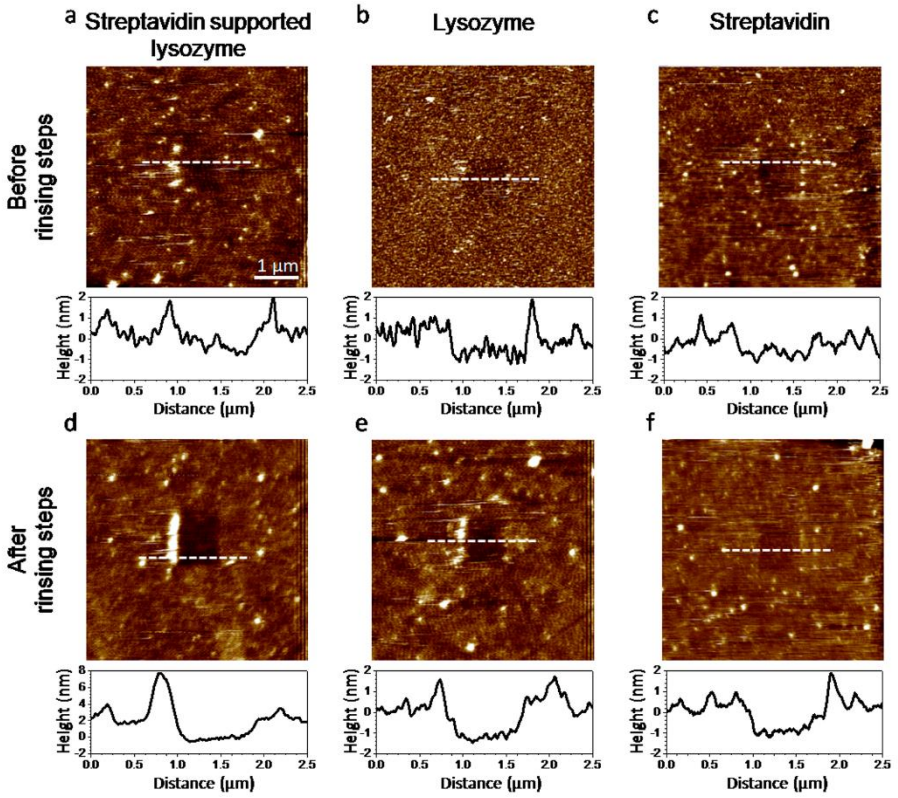

Figure S1. Topography of functionalized surfaces before and after rinsing steps. AFM height images (5 x 5 µm²; z scale = 5 nm) of surfaces functionalized with streptavidin-supported lysozyme (a, d), with covalently grafted lysozyme (b, e) and with covalently grafted streptavidin (c, f). Surfaces were imaged just after functionalization (a, b and c) or after 5 consecutive rinsing steps to mimic the washing steps applied between bacterial challenges (d, e and f). Vertical cross sections taken along the dashed lines and bridging the scratched squares are shown below the images. No significant differences were observed after rinsing steps indicating that protein layers are not removed over consecutive challenges.